INJURY ANALYSIS OF IMPACTS BETWEEN A CAGE-TYPE PROPELLER GUARD AND A SUBMERGED HEAD

Michael W. Scott
John J. Labra
Herbert Guzman
James V. Benedict
Harry Smith
James Ziegler

Biodynamic Research Corporation
9901 IH 10 West, Suite 1000
San Antonio, Texas 78230

ABSTRACT Propeller guards have been proposed for use on recreational and military boats. While the guards may prevent body contact with the spinning propeller, the potential of blunt trauma injury may become increasingly significant as impact speeds increase. In order to investigate the potential for blunt injury to the head in impacts between a propeller guard and a submerged head, a computer model of underwater impacts was developed and a series of underwater impact tests were performed. The computer model represents the human body as a multiple degree of freedom system. The physics of impacts in the underwater environment were mathematically modeled and underwater impacts between the head and a propeller guard were simulated with the computer model. In the impact tests series a Hybrid III anthropometric test device (ATD) was submerged in the head up position. A 115 HP outboard motor, equipped with a cage-type propeller guard, impacted the head of the ATD at speeds of 2.5 to 15.7 mph. Head accelerations and upper neck forces were measured. High speed film data were collected. Simulated and actual propeller guard impacts with the ATD head indicate that cervical spine damage and/or focal skull penetration may occur for impact speeds in excess of 10 mph. Head impacts with the side of the guard at speeds greater than 15 mph have a high probability of producing a concussion. The findings suggest that while the use of a propeller guard may be beneficial for low speed head impacts, the problem of blunt trauma injury at speeds greater than 10 mph would make the propeller guard counter-productive in reducing injuries.

INTRODUCTION In May of 1988 the U.S. Coast Guard requested the National Boating Safety Advisory Council (NBSAC) to assess the feasibility of using propeller guards to protect submerged individuals from spinning propellers on outboard motors. The NBSAC's report, presented on November 7, 1989, recommended that the Coast Guard take no regulatory action requiring guards on outboard motors.[1] One of the arguments presented against the use of propeller guards was that the "guards may prevent cuts from body contact with a propeller but substitute the potential of blunt trauma injury, which becomes increasingly significant at speeds over 10 mph." This research project was undertaken to better define the potential for blunt injury trauma to the submerged head when struck by a propeller guard.

The project was composed of a series of underwater impact tests and an analytical analysis. In the impact tests a Hybrid III Anthropometric Test Device (ATD) was submerged in a tank and struck with an outboard motor equipped with a propeller guard. The head motions and biomechanical forces were measured for impacts of different speeds. The analytical portion of the study produced a computer model that simulates impacts between a submerged head and propeller guard. The computer model uses a model of the human and the lower unit and incorporates the physics of impacts in the underwater environment to produce the impact simulations. Data from the impact tests were used to validate the computer model. This research was sponsored by Mercury Marine and Outboard Marine Corporation (OMC).

IMPACT TESTS The site for the underwater impacts was the Center for Research in Special Environments (Center) at the State University of New York at Buffalo in Buffalo, New York. The Center has a 200 feet (ft) circumference, 8 ft deep, 8 ft wide pool that surrounds a centrifuge that rotates on a 21 ft arm. A platform, which extends over the pool, can be attached to the centrifuge gondola and used to tow objects through the water at various speeds. A transom was attached to this platform and the outboard motor was mounted on the transom.

The motor was a 1990 Johnson 115 HP outboard motor which weighs 252 pounds (lb). The guard placed on the lower unit was a cage-type guard that was constructed of 5/16 in. diameter steel wire and weighed 14.25 lb (Brunswick Corporation Patent No. 4957459). The motor was not powered for the tests and no thrust was generated by the propeller. In order to duplicate the moment that the thrust generates around the pivot

This manuscript was received for review 24 March 1994 and was accepted for publication 18 July 1994.

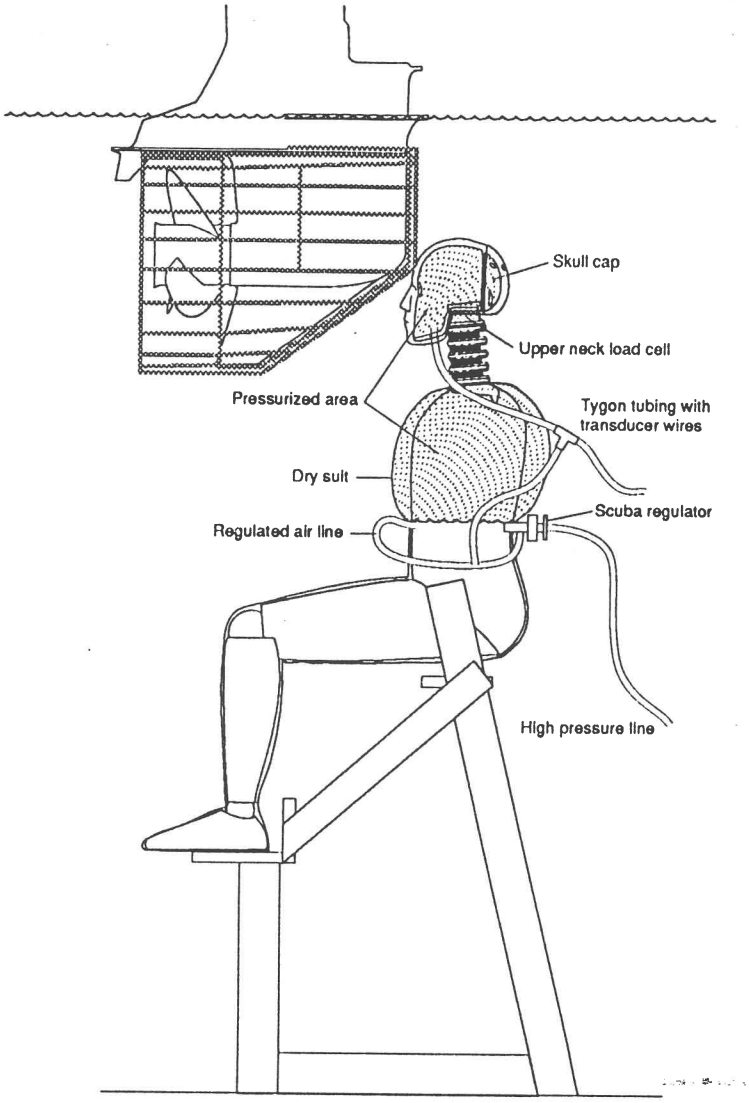

Figure 1. ATD Position in the Tank

tube, the hydraulic tilt mechanism was used to lower the motor. In the "down" position the tilt mechanism creates a moment about the pivot tube that is similar to the moment produced by the thrust of a planing boat.

A Hybrid III 50% male ATD (First Technology Safety Systems, Inc.) was used as a human surrogate. This ATD has a nominal height of 5 ft 9 in. and weight of 172 lb. Three linear accelerometers (Model No. 7231C-750, Endevco, Inc.) were mounted inside the head near the head's center of gravity (CG). An upper neck load cell (1716 load cell, R.A. Denton, Inc.) was mounted at the head/neck junction, an anatomical position equivalent to the occipital-condyle joint. This load cell measures the forces and moments applied by the neck to the head. The ATD was waterproofed with a dry suit and the head and upper torso were pressurized with air as shown in Figure 1. The ATD was weighted to give it a neutral buoyancy. Video cameras and a LOCAM® 16mm high speed camera took pictures through a window on the tank wall. A DAS-16F board (Keithley/Metrabyte, Inc.) mounted in an IBM Model 30 PC was used to collect the transducer data.

The ATD was held in position by means of nylon strings that were attached to a seat that was placed on the bottom of the tank. The clamps that held the nylon strings to the seat release under a load of less than one lb., so these attachments had no measurable effect on the motion of the ATD in the impacts. Because of its neutral buoyancy, the ATD actually floated over the seat as opposed to sitting on it (see Figure 1).

The centrifuge was accelerated forward at a constant rate until the lower unit reached the required tangential impact velocity. The motor trajectory during the period of contact with the ATD deviated from a straight line by less than .05 in.

All impacts were made with the ATD in the upright position as shown in Figure 1. This position placed the longitudinal axis of the neck perpendicular to the direction of travel of the guard. The guard impacted the head in the four different positions that are shown in Figure 2. Table I lists the impact speed and configuration for the seventeen impacts that were performed. Tests #1 and #2 were run with the ATD ¾ in. lower in the water than the other tests at Position A. In Position A the ATD's forehead was struck by the front vertical section of the guard. Since the projected frontal area of the guard is circular and the impact with the ATD's forehead occurred at the center of the projected area, these impact tests are referred to as centered tests. Position B is along the guard centerline, 3.5 in. lower than Position A. In Positions C and D the ATD remains at the same vertical position in the water as in the centered tests, but it is moved to the left of center approximately 6 in. and 8.5 in. respectively. Position D places the head in a position where it would miss the propeller blades, but still contact the guard. Impacts with the head in Positions B, C and D are referred to as off-center tests.

Table I.
Impact Speeds and Configurations

TEST #	IMPACT SPEED (mph)	HEAD POSITION
1	2.5	A
2,3,4	5.1	A
5,6	7.7	A
7,8	10.4	A
9,10	15.7	A
11,12	10.4	C
13,14	10.4	D
15,16	10.4	B
17	15.7	C

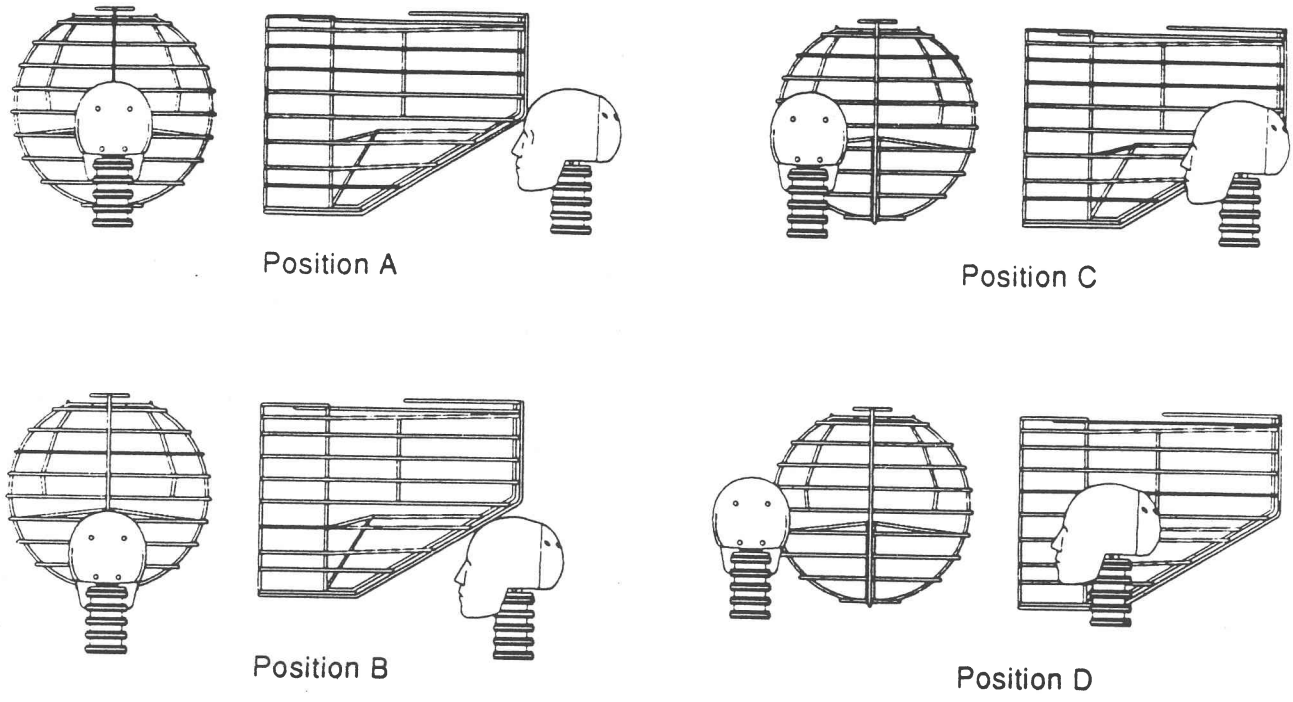

Figure 2. Position of the Head Relative to Guard for the Four Impact Positions

ANALYTICAL ANALYSIS The product of the analytical portion of the study was a computer model that can be used to simulate underwater impacts where the motion of the struck object is planar. The model uses a multiple degree of freedom mathematical model of the human body and subjects it to forces that are produced in an underwater impact. This model was validated by simulating the impacts that were performed at Position A (Tests #1 - #10).

The apparent inertial mass of a body accelerated in water is significantly increased because the water around it must also be accelerated. This apparent increase in mass is commonly referred to as added mass. Figure 3 is a simplified representation of added mass. A 10 lb. sphere is being accelerated by a swimmer. To the swimmer it feels like a 15 lb. sphere, since he must accelerate approximately 5 lbs. of water around the sphere as well as the 10 lb. mass of the sphere. For a cylinder and an ellipsoidal cylinder the added mass can be even greater, depending on the orientation of the longitudinal axis relative to the direction of acceleration.[2,3]

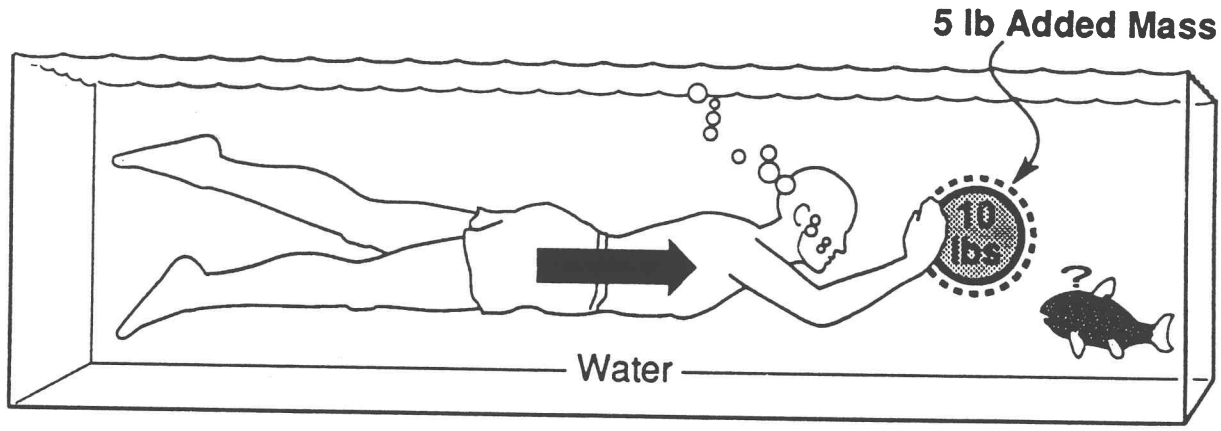

Figure 3. The 10 lb Sphere Feels Like a 15 lb Sphere When the Swimmer Starts to Push It Because of the Added Mass.

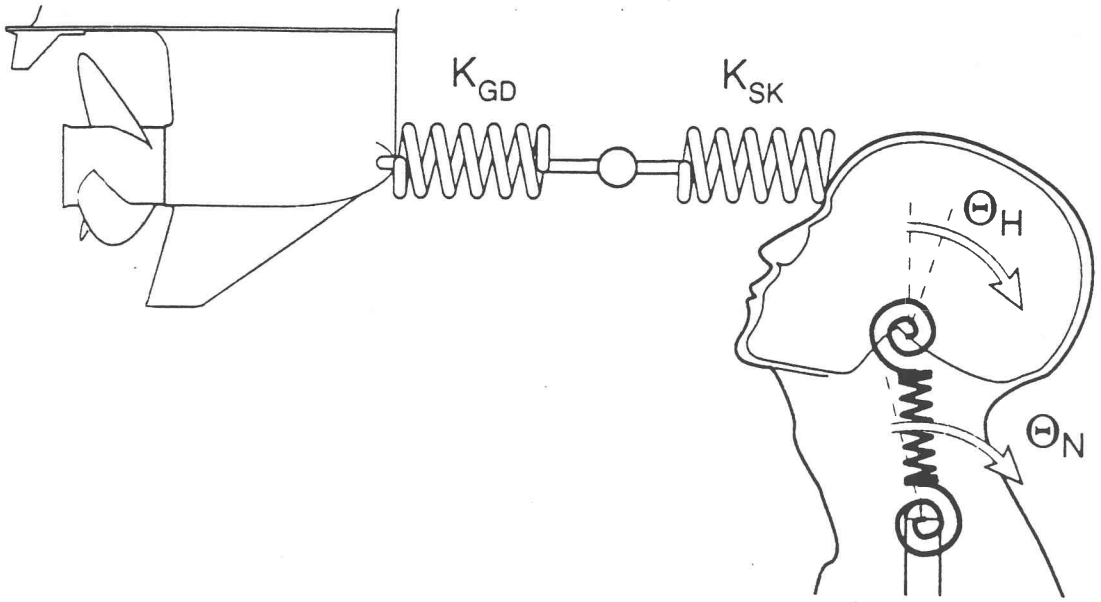

Figure 4. Schematic of the Human and Outboard Model Showing the Dynamic Elements of the Models

In addition to the added mass a moving submerged body will experience hydrodynamic drag. Typically drag is expressed by means of a drag coefficient, C_D, defined by the equation:

$$D = \frac{1}{2} C_D \rho V^2 S \qquad [1]$$

where S is the projected area of the body perpendicular to the direction of flow, V is the fluid velocity and ρ is the density of the fluid.[3] The drag coefficient is a function of the body shape, orientation and speed. The head, neck and thorax are the body segments that are included in the human model. The extremities are neglected as their mass has little effect on the biomechanical forces generated in the head and neck when the submerged head is impacted. The head, neck and thorax are geometrically idealized as a sphere, cylinder and an ellipsoidal cylinder respectively. The mass of each segment is determined from anthropometric data and is adjusted to simulate impacts on different size people.[4] During the simulated impacts, the added mass and hydrodynamic drag are taken into account for each of the body segments.

Schematic representations of the human body and outboard motor used in the model are shown in Figure 4. The model has linear torsional springs at the head/neck and neck/thorax junctions that resist rotation and dissipate energy (rotational damping). In the axial direction the neck is idealized by a spring and damper. The skull/skin is represented as a spring with a linear compliance (K_{SK}). The actual value used for each of the parameters is based on empirical data that represents human properties or, in the case of the test simulations, data for the Hybrid III ATD.[4]

The lower unit/guard is given an effective compliance (K_{GD}) by modeling a structure with a spring at the impact point. The outboard is given the mass and geometrical properties of the motor being used in the simulation. Due to the much larger weight of the boat and motor in comparison to the human head, the boat mass is not directly considered in the analysis as the assumption is made that the pre-impact velocity of the motor's attachment point with the boat, the pivot tube, remains constant.

The method of Lagrange is used to determine the motion of the segments of the human model during an impact. In terms of generalized coordinates the equations of motion are derived from the Lagrangian equations:

$$\frac{d}{dt}\left[\frac{\partial T}{\partial \dot{q}_i}\right] - \frac{\partial T}{\partial q_i} = Q_i \qquad [2]$$

where $T=T\ (q,\dot{q})$ is the kinetic energy of the system and Q_i are the generalized forces of the system. For the kinematics of the head, neck, thorax and lower unit seven generalized coordinates are used, i.e.,

$$(\theta_H, \theta_N, \theta_T, \theta_{OB}, X_H, Z_H, r_N) \qquad [3]$$

where: θ_H, θ_N, θ_T, are the rotational angles of the head (subscript H), neck (subscript N) and thorax (subscript T) that are shown in Figure 4;

Table II.
PARAMETERS USED IN SIMULATIONS

OUTBOARD IMPACT DATA
Total Weight: 265 lbs.
Mass Moment of Inertia: 149 lb-in-s²
CG to Motor Mount Location: 2.81 in.
Prop Centerline to CG Location: 26.80 in.

HYBRID III DATA*
Chin/Neck Interface Rotational Stiffness: 1266 in-lb/rad
Suprasternale Rotational Stiffness: 811 in-lb/rad
Chin/Neck Interface Rotational Damping: 13.2 in-lb-sec/rad
Suprasternale Rotational Damping: 0 in-lb-sec/rad
Neck Axial Stiffness: 3000 lb/in
Neck Axial Damping: 8.6 lb-sec/in

Head Weight: 11 lbs
Neck Weight: 3.8 lbs
Thorax Weight: 68 lbs

Head Mass Moment of Inertia: 0.28 lb-in-sec²
Neck Mass Moment of Inertia: 0.06 lb-in-sec²
Trunk Mass Moment of Inertia: 18.9 lb-in-sec²

Head Radius: 4.1 ins
Neck Radius: 2.5 ins
Thorax Radius: 6.4 ins
Neck Atlas to Head CG Distance: 2.1 ins
Neck Length: 4.5 ins
Trunk Length: 20.4 ins

* **Where data from Hybrid III ATD were not available, data were based on cadaver data.**

X_H, Z_H are the translational components of the head CG;
r_N is the radial extension of the neck;
and θ_{OB} is the rotational angle of the outboard (subscript OB) with respect to the attachment point within the boat.

The kinetic energy of the system is:

$$\begin{aligned} T = {} & +\tfrac{1}{2}M_H(\dot{X}_H^2+\dot{Z}_H^2)+\tfrac{1}{2}M_N(\dot{X}_N^2+\dot{Z}_N^2) \\ & +\tfrac{1}{2}M_T(\dot{X}_T^2+\dot{Z}_T^2)+\tfrac{1}{2}M_{OB}(\dot{X}_{OB}^2+\dot{Z}_{OB}^2) \\ & +\tfrac{1}{2}I_H\dot{\theta}_H^2+\tfrac{1}{2}I_N\dot{\theta}_N^2+\tfrac{1}{2}I_T\dot{\theta}_T^2+\tfrac{1}{2}I_{OB}\dot{\theta}_{OB}^2 \end{aligned} \qquad [4]$$

where: $\dot{X}_i$, $\dot{Z}_i$ $(i = H, N, T, OB)$ are the CG translational velocities of the head, neck, thorax and lower unit;
M_i $(i = H, N, T, OB)$ are the corresponding masses; and I_i $(i = H, N, T, OB)$ are the corresponding mass moment of inertia for the body segments and the lower unit.

The translational displacement components for the neck and thorax are related to the rotational degrees of freedom by:

$$\begin{aligned} X_N &= X_H - l_H\sin\theta_H - \tfrac{1}{2}l_N\sin\theta_N \\ Z_N &= Z_H - l_H\cos\theta_H + \tfrac{1}{2}l_N\cos\theta_N \end{aligned} \qquad [5]$$

$$\begin{aligned} X_T &= X_H - l_H\sin\theta_H - l_N\sin\theta_N - l_T\sin\theta_T \\ Z_T &= Z_H - l_H\cos\theta_H + l_N\cos\theta_N + l_T\cos\theta_T \end{aligned}$$

where (l_H, l_N, l_T) are the body segment lengths. With respect to be generalized forces Q_i on the right hand side of Equation [2] these include the following lower unit and anatomical properties:

- chin/neck rotational stiffness
- chin/neck rotational damping
- lower neck (C_7-T_1) rotational stiffness
- lower neck (C_7-T_1) rotational damping
- neck axial stiffness
- neck axial damping
- skull/skin compliance
- lower unit effective compliance
- lower unit mass and geometric properties

Substitution of the generalized forces along with the Equations [4] and [5] into Equation [2] results in a 6 X 6 matrix set of equations in the form of:

$$\left[A_{ij}\right]\begin{bmatrix} \ddot{\theta}_H \\ \ddot{\theta}_N \\ \ddot{\theta}_T \\ \ddot{r}_N \\ \ddot{X}_H \\ \ddot{Z}_H \end{bmatrix} = \left[B_i\right] \quad (i,j = 1 \text{ to } 6) \qquad [6]$$

Through the use of numerical methods, the associated body segment accelerations and biomechanical forces are uniquely solved as a function of time.

The computer model was used to simulate the centered tests. In order to simulate these impact tests the model inputs had to represent the Hybrid III ATD, and the outboard motor parameters had to represent a 1990 115 HP Johnson outboard motor. The pertinent parameters are given in Table II.

RESULTS FOR CENTERED TESTS In the 2.5 mph centered tests there is a single contact between the guard and the ATD's head. At impact speeds greater than 2.5 mph the head kinematics are composed of the three distinct phases that are shown in Figure 5. The first contact between the guard and the head, Phase I, is characterized by a high rearward acceleration and a

moderate downward acceleration of the head. The downward motion of the head is resisted by the neck as the neck is compressed. Surprisingly, the head goes into flexion relative to the upper neck during Phase I and a flexion moment is generated at the upper neck. All of the significant biomechanical forces are generated in Phase I.

The Phase I impact gives the head a rearward velocity greater than the lower unit, and the head is able to, at least momentarily, speed away from the guard. Once the head is completely disengaged from the guard, the start of Phase II, the head undergoes a rapid extension rotation. The combination of drag forces in the water and rotational motion of the head allow the guard to catch up with the head.

Phase III begins when the guard contacts the face again. The exact position of the head at the second impact in the centered tests depends on how far the head rotated during Phase II. Compared to the Phase I impact, the accelerations in this second impact are much less since the velocity difference between the guard and the head is smaller.

The impact force (F_I) that acts on the head was not directly measured in the tests but is estimated using the head accelerations and neck forces. In order to account for the added mass of the head, the head mass of 10.25 lb was multiplied by a factor of 1.5. Therefore:

$$\vec{F}_I = (-1.5M_H\vec{A}_H) + \vec{F}_N \qquad [7]$$

where $\vec{F}_I$ is the impact force, M_H is the mass of the head, $\vec{A}_H$ is the acceleration of the head and $\vec{F}_N$ is the force applied to the head by the neck. Table III lists the peak impact forces, the peak head accelerations, and the peak neck axial compression loads for the centered tests. (Note: No data was collected for Test #9). All of the peak values were measured in the Phase I impact. The centered tests performed at speeds greater than 5.1 mph produced high head impact forces and accelerations and high neck forces.

A surprising finding in the centered tests was the flexion moment that was developed in the upper neck during the Phase I impact. While the flexion moment was not large enough to produce an injury (325 in. lbs in Test #10), the presence of this moment demonstrates how the guard interaction with soft tissue may generate biomechanical forces away from the point of impact. The schematics in Figure 6 demonstrate how this flexion moment is thought to occur. Initially the impact causes the upper neck to translate rearward with the base of the skull, while the base of the neck remains relatively stationary. As the head moves rearward the neck wants to go into extension but the guard, which has penetrated into the rubber skin, prevents the head from rotating into extension. This places the neck in an unusual situation since it must maintain the connection between the rearward moving, non-rotating head and the stationary torso. The neck appears to accommodate the head and torso by having the upper neck go into flexion and the lower neck go into extension. Once the head is free of the guard, Phase II, the restraining force can no longer be applied and the head rapidly goes into extension. Because of the steel wire construction, the

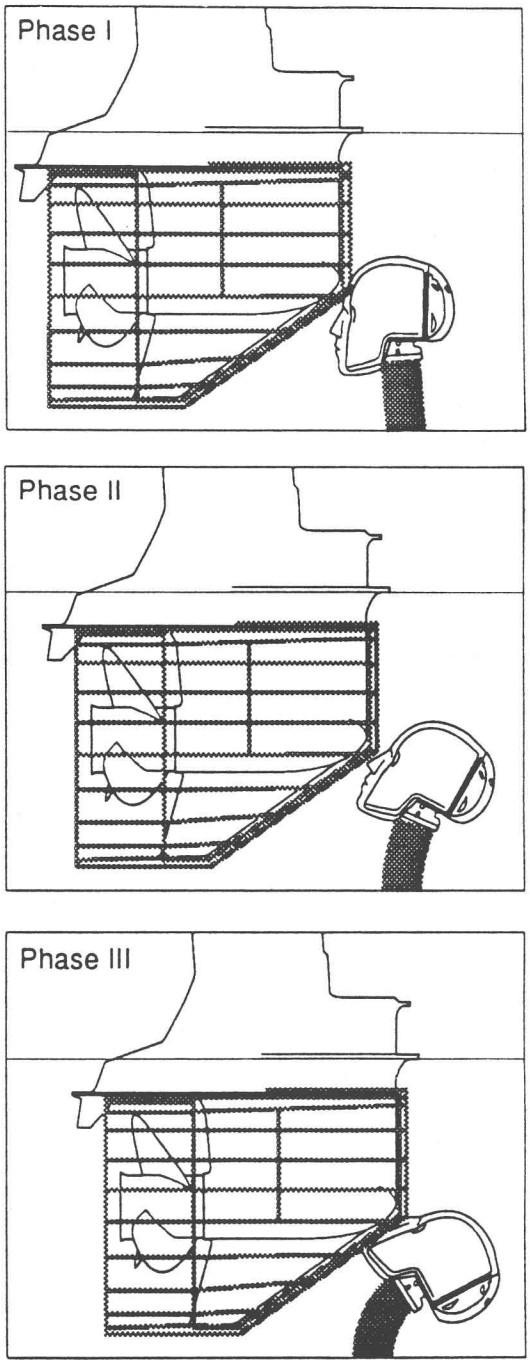

Figure 5. Overview of the Three Phases of Head Motion in the Centered Tests (Position A)

Table III. Peak Values in the Centered Impacts and Simulations

TEST # / IMPACT SPEED	IMPACT TESTS			SIMULATED IMPACTS		
	IMPACT FORCE (lb)	HEAD CG ACC. (g's)	NECK AXIAL LOAD (lb)	IMPACT FORCE (lb)	HEAD CG ACC. (g's)	NECK AXIAL LOAD (lb)
1 (2.5 mph)	187	7	125	175	10	90
2 (5.1 mph)	347	15	219	667	39	206
3 (5.1 mph)	643	37	284			
4 (5.1 mph)	662	38	251			
5 (7.7 mph)	2572	150	461	2202	127	420
6 (7.7 mph)	2431	142	433			
7 (10.4 mph)	4043	233	625	4111	237	611
8 (10.4 mph)	4579	260	605			
10 (15.7 mph)	5812	331	824	6154	353	822

guard appears to have the ability to fix the head orientation during engagement and prevent the head from rotating. This action appears to be the cause of the axial compression force that acts on the neck (see Table III).

Since the head motion in the centered tests is essentially two-dimensional, the analytical model was used to simulate these tests and the results of those simulations are also presented in Table III. An effective force angle with respect to the horizontal of 20° to 25° was used in the modeling analysis to describe the interface contour between the guard and the head as well as the engagement between the head and the guard. The results given in Table III are for an impact angle of 22.5°. The simulations produced peak head loads and accelerations and neck loads very similar to those measured in the tests.

RESULTS FOR OFF-CENTER TESTS The head impacted the guard from one to three times in each of the off-center tests. The actual number of head contacts varied with the impact position and speed. Since the initial contact between the head and the guard occurs farther back on the guard than in the centered tests (see Figure 2), the total time the guard and head are in contact is less than in the centered tests at the same impact velocity.

The guard struck the head in Position B in Tests #15 and #16 at 10.4 mph. In this position the head impacted the center sloping section of the guard (slope of approximately 30° to the horizontal). Like the centered tests, there were two distinct head impacts in these tests and the first always produced the more significant biomechanical forces. Tests #11 and #12 (10.4 mph) and Test #17 (15.7 mph) were conducted utilizing Position C. There were three distinct impacts between the guard and the ATD's head when the impact occurred with the ATD in Position C at an impact speed of 10.4 mph. After the third impact the head had moved laterally to the left enough to allow the guard to pass by. At the higher impact speed in Test #17, there were only two contacts. Tests #13 and #14 (10.4 mph) were conducted using Position D. In these tests there was only one contact between the guard and the ATD's head, the lateral velocity achieved by the head in this single impact carried it away from the guard.

The off-center tests produced lower forces than the centered tests at the same speed because of the reduced angle of the impacting surface (see Figure 2). The off-center tests also produced flexion moments in the upper neck that were thought to be due to engagement with the guard. Table IV gives the peak head impact forces, peak head accelerations and peak neck axial compression loads for the off-center tests. The tests at Position B produced high impact forces and compression neck loads. The forces and accelerations for the tests performed at Positions C and D were much lower. The forces at Position D were higher than those at Position C because the head's first contact with the guard was at the rear of the guard on the stiff ring that encircles the propeller.

In order to investigate the possibility of a closed head injury for impacts in Position C the lateral angular velocity and acceleration of the head are required. It is not possible to make an accurate measurement of the head angular motion from the photographic data so the

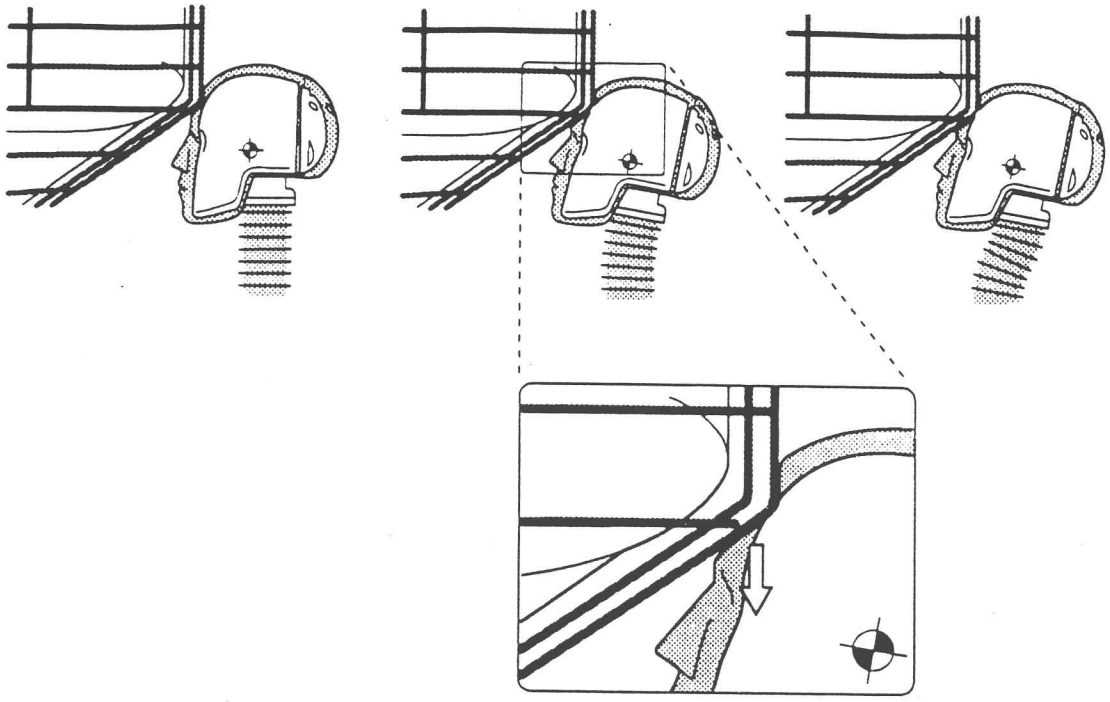

Figure 6. Guard Engagement with the Rubber Skin on the Forehead of the ATD in the Centered Impact. Arrow in the Blow-Up is the Downward Reaction Force Applied to the Head that Prevents the Head From Rotating.

measured lateral bending moments have been used to estimate the radial velocities and accelerations. At Position C the guard struck the head above the head CG and the resulting motion was a simple lateral flexion motion. It was not possible to use this technique to determine the lateral rotational motion at Position D because the guard impact occurred below the head CG and the head motion was too complex. The peak rotational velocities and accelerations are listed in Table V for impacts at Position C at 10.4 mph (Tests #11 and #12) and 15.7 mph (Test #17). These values occur shortly after the first impact. The rotational accelerations and velocities listed for Tests #11 and #12 are mean values for the two tests.

INJURY ANALYSIS An impact to the head can cause injury through the direct application of force, which fractures bone and destroys soft tissue, and by excessive acceleration of the brain, which causes an indirect form of head injury called a closed head injury. In a closed head injury the skull is accelerated by the impact and the skull in turn, attempts to accelerate the brain. Closed head injuries are the result of both translational and rotational accelerations of the skull. Diffuse axonal injuries (DAI) are thought to be caused primarily by rotational accelerations.[5]

Table IV. Peak Forces and Accelerations in the Off-Center Impacts

TEST #	HEAD POSITION	IMPACT SPEED (mph)	IMPACT FORCE (lb)	HEAD CG ACC. (g's)	NECK AXIAL LOAD (lb)
11	C	10.4	389	19	101
12	C	10.4	345	20	114
13	D	10.4	446	26	40
14	D	10.4	545	27	45
15	B	10.4	970	40	755
16	B	10.4	1130	35	851
17	C	15.7	537	30	184

Table V. Peak Rotational Velocities and Accelerations

TEST #	POSITION	IMPACT SPEED (mph)	PEAK ROTATIONAL VELOCITY (rad/sec)	ROTATIONAL ACCELERATION (rad/sec^2)
11.12	C	10.4	40.0	8,800
17	C	15.7	67.0	9,900

Studies that have measured the force required by narrow cylindrical impactors to break the frontal bone indicate that the mean fracture force is approximately 1480 lbs.[6,7] These narrow impactors produce depressed skull fractures. Based on this criterion the centered tests that occur at speeds equal to or greater than 7.7 mph have a high probability of producing depressed frontal bone fractures (see Table III). For impacts at Position B, the peak impact forces generated in the 10.4 mph impact (Tests #15 and #16) are close to but below this criterion, but at impacts speeds greater than 10.4 mph there is a high probability of a depressed skull fracture.

The Head Injury Criterion (HIC) is used by the National Highway Transportation Safety Association (NHTSA) to determine the potential for a closed head injury due to translational acceleration of the skull.[8] The equation for calculating the HIC is based on the magnitude and the duration of the acceleration and NHTSA uses a HIC value of 1000 as a pass-fail criteria in setting vehicle safety standards. Based on the HIC injury criteria of 1000, only the 15.7 mph centered impacts (Tests #9 and #10) would produce a HIC value greater than 1000. Of course if the skull fractured the acceleration values and the resulting HIC would be less, although a brain injury would still occur.

A criterion for DAI type head injuries is given as a function of the angular velocity and acceleration.[9] Based on this criterion the impact in Test #17 has a high probability of producing a severe concussion. Loss of consciousness in an accident on land is a serious injury, but it is usually not an immediate threat to life. In the water environment loss of consciousness is a life-threatening event because of the possibility of drowning. Head impacts on the side of the guard at speeds greater than or equal to 15.7 mph have a high probability of producing a loss of consciousness.

One criterion for neck compression injuries has been developed by exposing the Hybrid III ATD to human injury producing conditions.[10] This neck injury criterion is a function of the duration and the magnitude of the compressive load. Tests #10, #15 and #16 would produce compression loads that come close to injury levels but do not exceed this criterion. Based on this criterion, there is a high probability of a severe neck compression injury for head impacts in Position A at impact speeds greater than 15.7 mph and for head impacts in Position B at impact speeds greater than 10.4 mph.

CONCLUSION The results of this study support the argument of the NBSAC report that blunt trauma injuries may become significant at speeds greater than 10 mph. For a limited low speed impact range, approximately 10 mph and less, a propeller guard on a lower unit that impacts a submerged head may mitigate injuries. The degree of protection depends on the size and weight of the individual, lower unit size, the impact site on the guard and the anatomical area struck as well as the body's orientation in the water.

Over 80% of the boating fatalities included in the U.S. Coast Guard's accident category "Struck by Boat or a Propeller" occur at planing speeds, 15 mph or greater for most recreational boats.[1] The results of this study indicate that impacts between a submerged head and a guard on a lower unit travelling at these speeds would most likely produce severe head and neck injuries. At these impact speeds, it is difficult to prevent injury for individuals who are struck by a portion of the boat's lower unit, be it a propeller or a guard.

This test protocol had the ATD in an upright position which reduced the probability of neck injury but the engagement action of the guard still caused high neck loads to be produced. If the torso was more pitched forward when the impact occurred, a position more like that of a swimmer, the impact would have to move some of the torso mass out of the path of the lower unit as well as the head and neck. The forces required to move the torso would be applied through the neck, thus the probability of neck injury would increase as the torso was pitched more forward.

The engagement action may occur in impacts to other areas of the body when the steel wires of the guard engage the soft tissue of the impacted area. This engagement may cause high biomechanical forces to be generated at sites away from the impact site by preventing the impacted area from rotating out of the path of the guard.

Impacts to the side of the guard at speeds greater than 15 mph may produce a loss of consciousness. The

possibility of head contact on the side of the guard is enhanced with the increase in projected frontal area that occurs with the placement of a guard on the lower unit. Figure 7 shows that the guard used in these tests (O.D. 16.325 in.) presents a total frontal surface area of 211 sq. in., which is 53% greater than the 138 sq. in. area transcribed by the 13.25 in. propeller.

This study has also demonstrated that a mathematical modeling approach to a rather complex dynamic and kinematic problem can be utilized as a cost effective and technically sound approach in addressing underwater impacts. The model can readily be adapted to investigate impacts to other parts of the body such as the limb and torso. The model also helps to provide insight into the biomechanical forces that cannot be directly measured in the experimental tests.

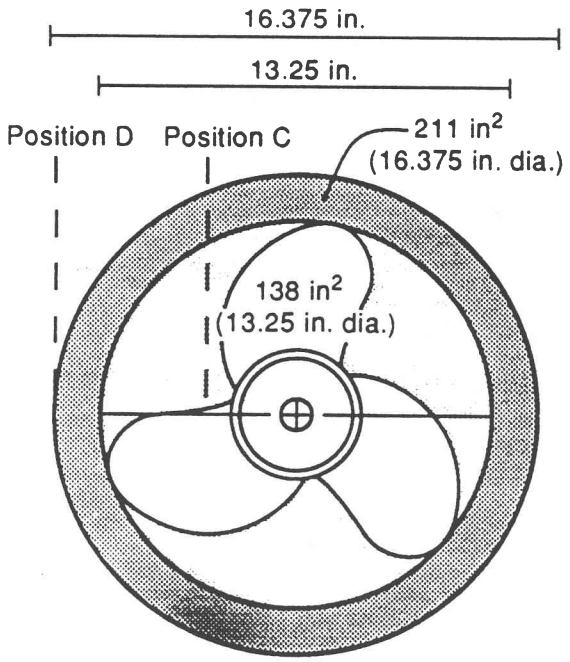

Figure 7. Increase in Projected Frontal Area with the Addition of the Propeller Guard

REFERENCES

1. Getz, James E., et al, Report of the Propeller Guard Subcommittee: The National Boating Safety Advisory Council, November 1989.

2. Birkhoff, G., Hydrodynamics: Princeton University Press, 1960.

3. Chung, H. and Chen, S.S., Hydrodynamic Mass: 1984 ASME Pressure Vessels and Piping Conference.

4. Bowman, B. M., et al, Simulation Analysis of Head and Neck Responses: SAE Paper No. 841668.

5. Gennarelli, T.A., et al, Diffuse Axonal Injury and Traumatic Coma in the Primate: ANN Neurol, Vol. 12, pp. 564-574, 1982.

6. Hodgson, V.R., et al, Fracture Behavior of the Skull Frontal Bone Against Cylindrical Surfaces: SAE Paper No. 700909, Fourteenth Stapp Car Crash Conference Proceedings, 1970.

7. Hodgson, V.R., et al, Strength of the Human Skull v. Impact Surface Curvature: DOT Contract No. DOT-HS-146-2-230, Report No. HS-801 001, Nov. 1973.

8. Human Tolerance to Impact Condition as Related to Motor Vehicle Design: SAE J885, 1986.

9. Gennarelli, T.A., et al, Clinical Rationale for a Head Injury Angular Acceleration Criterion: Association for the Advancement of Automotive Medicine, October 4, 1989, Washington, D.C.

10. Mertz, H.J., et al, An Assessment of Compressive Neck Loads Under Injury Producing Conditions: The Physician and Sports Medicine, Vol. 6, No. 11, Nov. 1978.

BIOGRAPHY OF DR. MICHAEL W. SCOTT

Dr. Michael W. Scott is a consulting engineer at Biodynamic Research Corporation (BRC) in San Antonio, Texas. BRC performs analysis in the areas of accident reconstruction and injury reconstruction, as well as research related to human acceleration tolerances and injury events. Dr. Scott received his M.S. and Ph.D. (Engineering Science) from the University of Buffalo and did an NIH Post-Doctoral Fellowship in the University of Buffalo Physiology Department. Previously, Dr. Scott worked at KRUG International as a Research Engineer in the development of Chemical Defense Collection Protection Systems. Prior to this, he was the manager of the Engineering Test Lab at Scott Aviation in Lancaster N.Y.

BIOGRAPHY OF DR. JOHN LABRA Dr. Labra's academic background includes a B.S. and M.S. in Aeronautics and Astronautics at New York University. He received a Ph.D specializing in Engineering Mechanics at New York University in 1973. His professional background since 1973 includes 9 years at Southwest Research Institute in San Antonio, Texas, involved in vehicular and highway safety. Since 1985, Dr. Labra has been the president of Computech Engineering Inc. in San Antonio, Texas, and he is affiliated with Biodynamic Research Corporation in San Antonio. Since 1985, he has been maintaining a consulting practice specializing in the fields of Biomechanics, Occupant Kinematics, Injury Causation and Vehicle Crashworthiness.